

Journal of Materials Chemistry A

Accepted Manuscript



This is an *Accepted Manuscript*, which has been through the Royal Society of Chemistry peer review process and has been accepted for publication.

Accepted Manuscripts are published online shortly after acceptance, before technical editing, formatting and proof reading. Using this free service, authors can make their results available to the community, in citable form, before we publish the edited article. We will replace this *Accepted Manuscript* with the edited and formatted *Advance Article* as soon as it is available.

You can find more information about *Accepted Manuscripts* in the [Information for Authors](#).

Please note that technical editing may introduce minor changes to the text and/or graphics, which may alter content. The journal's standard [Terms & Conditions](#) and the [Ethical guidelines](#) still apply. In no event shall the Royal Society of Chemistry be held responsible for any errors or omissions in this *Accepted Manuscript* or any consequences arising from the use of any information it contains.

Cite this: DOI: 10.1039/c0xx00000x

www.rsc.org/xxxxxx

ARTICLE TYPE

Promising alkoxy-wrapped porphyrins with novel push–pull moieties for dye-sensitized solar cells

Ming-Dao Zhang,^a Zi-Yang Zhang,^b Zhong-Qiu Bao,^c Ze-Min Ju,^a Xing-Yong Wang,^b He-Gen Zheng^{*a}, Jing Ma^{*b} and Xing-Fu Zhou^c

Dedicated to Professor Xinquan Xin on the occasion of his 80th birthday

Received (in XXX, XXX) Xth XXXXXXXXX 200X, Accepted Xth XXXXXXXXX 200X

DOI: 10.1039/b000000x

Dye-sensitized solar cells (DSSCs) have been considered as very promising third generation solar cells. Porphyrins are promising candidates as highly efficient sensitizers for DSSCs because of their superior light-harvesting ability in the visible region and mimicking photosynthesis. This paper focuses on the structure modification of porphyrin dyes for efficient DSSCs, which was based on the rational design with density functional theory (DFT) before the experiment. We synthesized and fully characterized four porphyrin dyes, named ZLD13, ZLD14, ZLD15 and ZLD16. On the one hand, we used 5-ethynylthiophene-2-carboxylic acid to replace 4-ethylbenzoic acid as the electron-withdrawing anchoring groups for the first time. Property study indicates that aggregation of porphyrin molecules can be suppressed sufficiently via this modification. On the other hand, 4,4'-di(2-thienyl)triphenylamine moiety, which has been proved to be a electron donor group for triarylamine dyes in our previous reports, were introduced to porphyrin dyes, and energy conversion efficiencies (η) were improved by 76% (ZLD15 VS ZLD13). After the two modifications, energy conversion efficiency (η) of ZLD16 is comparable with N719-based reference cell under the same conditions. Enhancement of photovoltaic performances from ZLD13 to ZLD16 is partly due to the decreased dark current and charge recombination rate.

1. Introduction

Dye-sensitized solar cells (DSSCs) are currently under intense academic and industrial investigations due to their low-cost fabrication and high power conversion efficiency.¹ During the process of photon to current in a DSSC device, photosensitizer acts as a key role determining the solar-cell performance.² Porphyrin sensitizers have drawn great interest because of their excellent light-harvesting function and mimicking photosynthesis.³ Moreover, recent developments on porphyrin-based solar cells exhibit a promising advance with the progress curve showing a feature of exponential rise.⁵

Recently, porphyrin ring with a 4-ethylbenzoic acid at its meso position has been demonstrated as an excellent platform for high efficiency DSSCs.⁵ In 2009, Diau et al. initially found that introducing bulky tert-butyl groups into phenyl groups increased the energy conversion efficiency (η) from 2.5% to 3.29%.⁵ In 2010, Bessho et al. added bis(4-hexylphenyl)amine to the porphyrin ring and increased the efficiency to 11%.⁶ In 2011, Yella et al. further replaced the tert-butyl groups by long alkoxy groups and a record efficiency of 12.3% was achieved.⁷

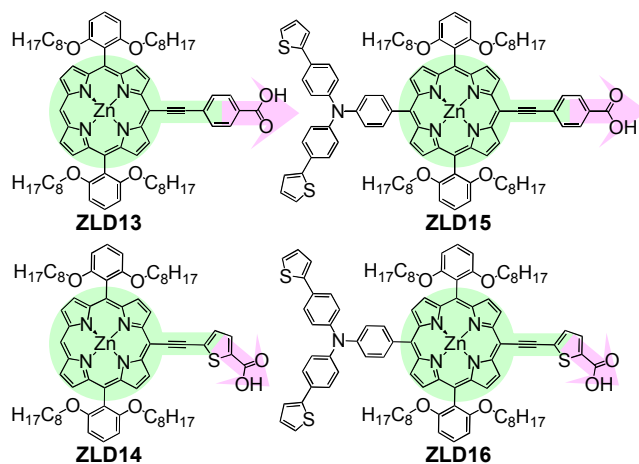
Although porphyrin-sensitized solar cells have obtained high efficiency now, there is still plenty room for us to reach the theoretical highest efficiency. One drawback of porphyrins for DSSCs is that their planar molecules often arrange orderly and closely on the nanocrystalline titanium dioxide film, therefore leading to dye aggregation.⁸ When 4-ethylbenzoic acid was introduced to porphyrin ring at its meso position (ZLD13,

Scheme 1), porphyrin ring would be located in the central axis of the electron acceptor. Then, the molecules would arrange orderly and aggregate on the semiconductor surface. Dye aggregation would inevitably lead to the reduction of electron injection efficiency and energy conversion efficiency, therefore, it's significant for us to avoid unfavorable dye aggregation in DSSCs through optimization of the molecular structure of the dye.

Herein, we report a novel electron-withdrawing anchoring group named 5-ethynylthiophene-2-carboxylic acid for porphyrin-sensitized solar cells. Different from 4-ethylbenzoic acid, when 5-ethynylthiophene-2-carboxylic acid was introduced to porphyrin ring, porphyrin ring would depart from the central axis of the electron acceptor, then the ordered arrangement of dye molecules would be destroyed and aggregation would be suppressed. On the basis of theoretical calculation, we firstly synthesized two fundamental porphyrin dyes, ZLD13 and ZLD14, containing 4-ethylbenzoic acid and 5-ethynylthiophene-2-carboxylic acid as the electron-withdrawing anchoring groups respectively. Photovoltaic performance tests further supported our design idea. The energy conversion efficiency (η) of ZLD14 is 5% higher than the efficiency of ZLD13.

Recently, we developed a new kind of electronic donor moiety named 4,4'-di(2-thienyl)triphenylamine moiety, and demonstrated that using suitable heterocyclic groups to modify the structures of triarylamine units may improve the electron donating ability.⁹ On the basis of theoretical calculation, we

found electron donating ability of 4,4'-di(2-thienyl)triphenylamine moiety may be favorable to enhance the performance of porphyrin-sensitized solar cells. Then, we introduced 4,4'-di(2-thienyl)triphenylamine moiety into porphyrin dyes ZLD13 and ZLD14, and obtained two new porphyrin dyes ZLD15 and ZLD16.¹⁰



Scheme 1 Molecular structures of ZLD13, ZLD14, ZLD15 and ZLD16.

ZLD13, ZLD14, ZLD15 and ZLD16 were employed as sensitizers in DSSCs. In order to evaluate the photovoltaic properties of the four dyes objectively, we employed N719 as the reference dye and manufactured the reference cell. Then, the photovoltaic performances of the devices under irradiation of AM 1.5G full sunlight (100 mW/cm²) were investigated in details.

Photovoltaic tests demonstrate that higher DSSCs' performance can be achieved after introducing 5-ethynylthiophene-2-carboxylic acid or 4,4'-di(2-thienyl)triphenylamine moiety to porphyrin ring (ZLD14 and ZLD15) compared to dye ZLD13. When 5-ethynylthiophene-2-carboxylic acid and 4,4'-di(2-thienyl)triphenylamine moiety were introduced to porphyrin ring (ZLD16) simultaneously, the DSSCs' performance was enhanced further. To explain the results, series of properties (such as dark current and electrochemical impedance spectroscopy) were investigated, laying a special emphasis on the energetics, and charge transfer processes at the dye/titania/electrolyte interface.

2. Results and discussion

Design and synthesis

Design of dyes is directed by theoretical calculations within the framework of DFT. The ground states of dyes were optimized by DFT with the 6-31G(d) basis sets for light elements and the LANL2DZ effective core potentials for Zn and Ti atoms. The vertical excitation energies of the low-lying states were then calculated by using the time dependent density functional theory (TDDFT). All the calculations were carried out using Gaussian 09 program.¹¹ To test the influence of the density functional, we adopted M062X, CAM-B3LYP, B3LYP and wB97, respectively, to simulate the UV-vis absorption spectrum of ZLD13 (Fig. S1, Supporting Information). After that, dye ZLD13 was synthesized and its experimental UV-vis absorption spectrum was recorded to validate the calculation results. Four different functionals gave qualitatively coincident results with the experiments, and among them the UV-vis absorption spectrum simulated by B3LYP is rather close to experimental data. Therefore,

B3LYP was selected in the following calculations of other dyes, ZLD14~ZLD16.

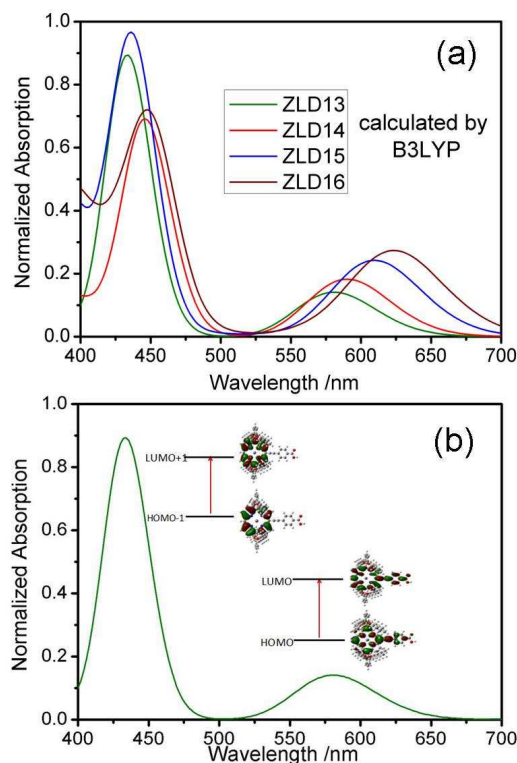


Fig. 1 (a) Simulated UV-vis absorption spectra of ZLD13~ZLD16 using TDDFT with B3LYP functional. (b) Assignment of absorption peaks (ZLD13 for example).

The calculated the UV-vis absorption spectra of ZLD13~ZLD16 are shown in Fig. 1a. The absorption spectra exhibit a red-shifted trend from ZLD13 to ZLD16, which indicates the improvement of light-harvest ability from ZLD13 to ZLD16.

According to the B3LYP calculation results, absorption peaks of dyes in the 400 to 500 nm and 520 to 660 nm ranges can be mainly assigned to the transition of HOMO-1→LUMO+1 and HOMO→LUMO, respectively (taking ZLD13 for example in Fig. 1b).

As shown in Table S1 (Supporting Information), both HOMO (highest occupied molecular orbital) and LUMO (lowest unoccupied molecular orbital) of ZLD13 (or ZLD14) are mainly π and π^* orbitals, respectively, which hover over the porphyrin ring and aromatic acid group. The HOMOs of ZLD15 and ZLD16 are almost populated over the whole conjugated systems, while the LUMOs of ZLD15 and ZLD16 are just delocalized in the porphyrin ring and the aromatic acid group. Charge-transfer transition can be observed from HOMO to LUMO of ZLD15 (or ZLD16).

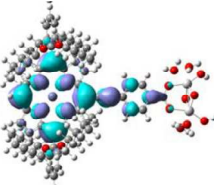
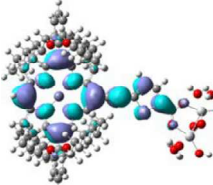
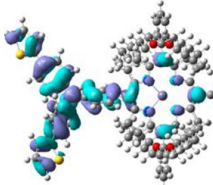
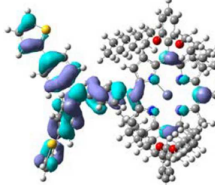
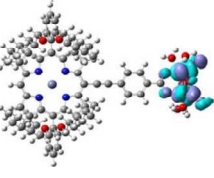
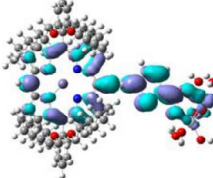
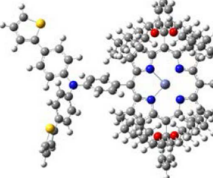
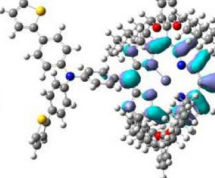
B3LYP calculation shows that the HOMO-LUMO gaps (ΔE) of ZLD13 (2.52 eV), ZLD14 (2.45 eV), ZLD15 (2.43 eV) and ZLD16 (2.30 eV) reveal a trend of gradual decrease (Table S2, Supporting Information), which is consistent with the calculated UV-vis absorption spectra of ZLD14~ZLD16 in Fig. 1a.

When a binuclear titanium model, $[\text{Ti}_2\text{O}_2(\text{OH})_2(\text{H}_2\text{O})_4]^{2+}$,¹² was used to mimic the TiO₂ nanoparticles, ZLD13~ZLD16 connecting the models are named as ZLD13-Ti~ZLD16-Ti. It was found that two carboxylic oxygen atoms bind to two

neighboring Ti atoms (Table 1). Like before, HOMOs of ZLD13-Ti and ZLD14-Ti are located at porphyrin ring and the aromatic acid group, whereas LUMO of ZLD13-Ti is populated in the binuclear titanium cluster, and LUMO of ZLD14-Ti partly transfers to the titanium model. HOMOs of ZLD15-Ti and ZLD16-Ti mainly are populated in 4,4'-di(2-thienyl)triphenylamine moiety, while LUMO of ZLD15-Ti is populated in the binuclear titanium cluster, and LUMOs of

ZLD16-Ti is delocalized over the porphyrin ring and the titanium model. A strong coupling between porphyrin dyes ZLD13~ZLD16 and TiO₂ nanoparticles, and obvious charge-transfer transition can be observed from HOMO to LUMO of all the four dyes after anchored on TiO₂.

Table 1 Frontier molecular orbitals (LUMO, HOMO) of ZLD13~ZLD16 after absorbed on the [Ti₂O₂(OH)₂(H₂O)₄]²⁺ model.^a

Dye	ZLD13-Ti	ZLD14-Ti	ZLD15-Ti	ZLD16-Ti
HOMO				
LUMO				

^a The calculations were carried out under vacuum using the 631-g(d) basis set and B3LYP functional (see ESI† of supporting information for details).

Therefore, red shift of UV-vis absorption spectra and evident charge separation and charge migration all suggest that photovoltaic performance of porphyrin-sensitized solar cells would be improved when 5-ethynylthiophene-2-carboxylic acid or 4,4'-di(2-thienyl)triphenylamine moiety were introduced to ZLD13. We synthesized the dye ZLD14-ZLD16, and the experimental details are shown in ESI† of supporting information.

Electronic absorption spectroscopy

Absorption spectra of these four porphyrin dyes measured in chloroform are shown in Fig. 2a, and Table 2 lists the corresponding spectral properties. All of four porphyrins exhibit maxima in the 400 to 500 nm and 520 to 660 nm ranges, corresponding to the Soret and Q bands, respectively. Absorption peaks (λ_{max}) for ZLD13 in CHCl₃ are at about 442 nm ($\epsilon = 168 \times 10^3 \text{ M}^{-1} \text{ cm}^{-1}$) in the Soret band, 565 nm ($\epsilon = 7.1 \times 10^3 \text{ M}^{-1} \text{ cm}^{-1}$) and 619 nm ($\epsilon = 8.6 \times 10^3 \text{ M}^{-1} \text{ cm}^{-1}$) in the Q band. After replacing the electron-withdrawing anchoring group with 5-ethynylthiophene-2-carboxylic moiety (ZLD14), the absorption peaks are red-shifted, due to the enhanced electron attracting ability. After introducing 4,4'-di(2-thienyl)triphenylamine moiety (ZLD15), the absorption peaks are also red-shifted, attributing to the enhanced electron donating ability. When the above two design policies are both applied (ZLD16), the absorption peaks are red-shifted further. The shifting trend of ZLD13~ZLD16's absorption peaks is consistent with the theoretical calculation result as shown in Fig. 1a.

Fig. 2b shows the absorbance profiles of the dyes anchoring on TiO₂ nanoparticle film. A bit broadening of the absorption spectra of dyes after anchoring on TiO₂ are reasonable and might be due to dye-TiO₂ interactions, dye-dye interactions, or both of them on the TiO₂ surface.^{13,14}

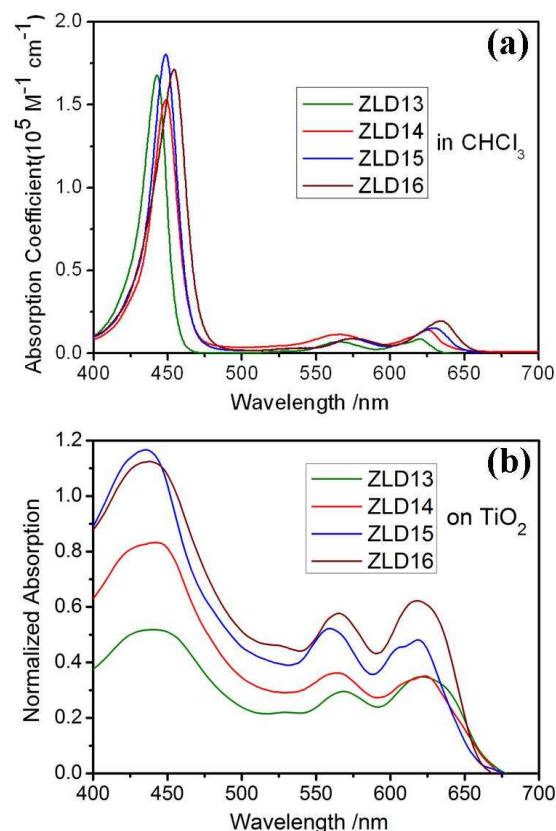


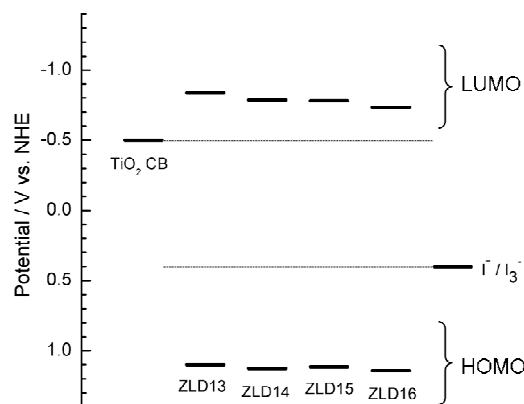
Fig. 2 (a) Electronic absorption spectra of ZLD13~ZLD16 dissolved in chloroform ($1.0 \times 10^{-6} \text{ M}$); (b) Absorption spectra of the dyes anchoring on the 12 μm porous TiO₂ nanoparticle films.

Table 2 UV-vis absorption properties of dyes dissolved in CHCl_3 .

Dye	Soret band [$\lambda_{\text{max}}/\text{nm}$ ($\epsilon \times 10^3 \text{ M}^{-1} \text{ cm}^{-1}$)]	Q band [$\lambda_{\text{max}}/\text{nm}$ ($\epsilon \times 10^3$ $\text{M}^{-1} \text{ cm}^{-1}$)]
ZLD13	442 (168)	565 (7.1), 619 (8.6)
ZLD14	449 (153)	566 (11.5), 625 (14.2)
ZLD15	449 (181)	574 (9.0), 629 (15.4)
ZLD16	454 (171)	575 (9.0), 634 (19.6)

Electrochemical studies

Quasi-reversible oxidation and reduction waves (E_{ox} and E_{red} in Table S3) were recorded for dyes ZLD13, ZLD14, ZLD15 and ZLD16 in the cyclic voltammetry (CV) measurements (Fig. S2).

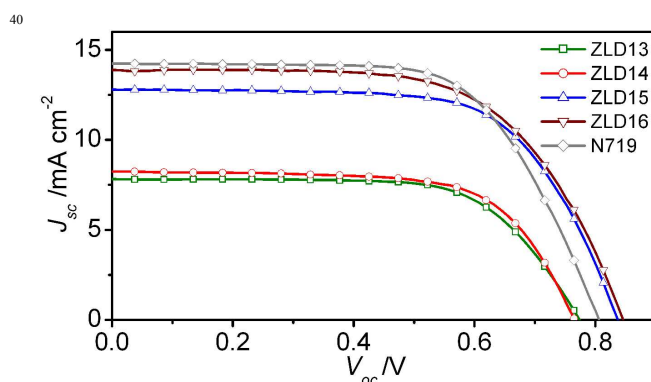
**Fig. 3** Potential-level diagram of the ZLD13–ZLD16 porphyrins, the TiO_2 conduction band, and the redox mediator.

The zero-zero excitation energy ($E_{0,0}$) estimated from the absorption onset and the ground-state oxidation potential (E_{ox}) were used to calculate the excited-state oxidation potential (E_{ox}^*). On the one hand, the deduced E_{ox}^* values of ZLD13–ZLD16 are more negative than the conduction band edge of the TiO_2 (-0.5 V vs NHE),¹⁵ indicating that the electron injection process should be energetically favorable. On the other hand, the ground-state oxidation potentials (E_{ox} in Table S3) of these four dyes are more positive than the redox potential of the I^-/I_3^- couple (0.4 V vs NHE),¹⁵ suggesting that the oxidized dyes should be able to accept electrons from I^- thermodynamically for effective dye regeneration. Consequently, all four dyes have enough thermodynamic driving forces for efficient DSSCs using nanocrystalline TiO_2 photoanode and I^-/I_3^- electrolyte (Fig. 3).

The experimental value of four dyes' band-gaps reveal a trend of gradual decrease [ZLD14 (1.938 V) > ZLD13 (1.911 V) > ZLD15 (1.893 V) > ZLD16 (1.877 V)], which is consistent with theoretical calculation results.

Photovoltaic performance of DSSCs

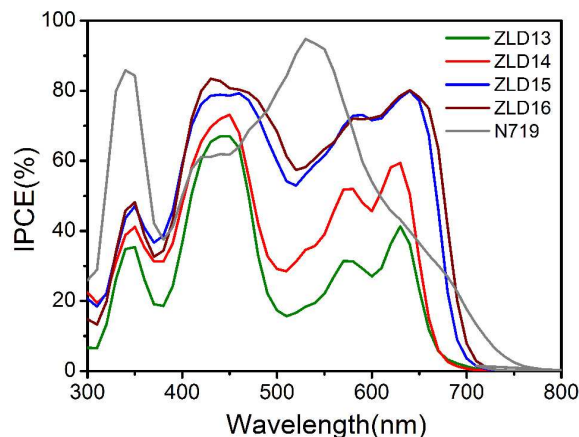
These four dyes were used to manufacture dye-sensitized solar cells. The devices employed FTO glass anchored dye-loaded TiO_2 nanoparticle film as positive electrode,¹⁶ platinum-coated glass as counter electrode,¹⁶ and a solution of 0.6 M DMII, 50 mM LiI, 30 mM I_2 , 0.5 M tert-butylpyridine and 0.1 M GuNCS in acetonitrile and valeronitrile (85 : 15) as the electrolyte.¹⁷ Photocurrent-voltage (J - V) curves for the DSSCs were recorded under irradiation of AM 1.5G full sunlight (100 mW/cm^2) and presented in Fig. 4.¹⁸ The exact results are summarized in Table 3.

**Fig. 4** Photocurrent density-voltage curves for the DSSCs based on ZLD13–ZLD16 and N719 under irradiation of AM 1.5G full sunlight.**Table 3** Photovoltaic parameters of the J - V curves for the DSSCs under irradiation of AM 1.5G sunlight.^a

Dye	Dye adsorbed amounts ($10^{-7} \text{ mol}/\text{cm}^2$)	V_{oc} (V)	J_{sc} (mA/cm^2)	FF (%)	η (%)
ZLD13	3.1	0.769	7.81	66.89	4.02
ZLD14	2.3	0.762	8.24	66.92	4.20
ZLD15	3.8	0.838	12.80	65.97	7.08
ZLD16	2.8	0.847	13.88	62.67	7.37
N719	2.5	0.806	14.23	64.80	7.43

^a The size of the active area for each cell was $4 \times 4 \text{ mm}$.

Among the fabricated PSSCs, the energy conversion efficiency (η) of N719 reaches the maximum value of 7.43%. The energy conversion efficiencies (η) of ZLD14 (4.20%) is 4.5% higher than that of ZLD13 (4.02%) because of the enhancement of J_{sc} values from ZLD13 to ZLD14. Both V_{oc} and J_{sc} of ZLD15 are significantly greater than those of ZLD13, leading to 76% enhancement of the overall power conversion efficiency for the two devices (7.08% vs. 4.02%). Enhancement of J_{sc} values from ZLD15 to ZLD16 results in the further improvement of energy conversion efficiency. ZLD16 reaches the energy conversion efficiency (η) of 7.37%, which is comparable with N719. The above results directly demonstrate that the photovoltaic performance of porphyrin dye can be improved after introducing 4,4'-di(2-thienyl)triphenylamine moiety, or replacing the electron-withdrawing anchoring group with 5-ethynylthiophene-2-carboxylic moiety.

**Fig. 5** IPCE of DSSCs based on ZLD13–ZLD16 and N719.

The incident photon-to-current conversion efficiency (IPCE) data of these dyes was collected and presented in Fig. 5.

curves of four porphyrin dyes have the similar profiles. IPCE values of ZLD16 exceed 60% from 410 to 520 nm, with a maximum value (83.0%) at 440 nm. IPCE curve of ZLD13-ZLD15 are lower and narrower than that of ZLD16 with different degrees. The estimated J_{sc} values from IPCE data are 7.48, 8.07, 12.5, and 13.27 mA/cm² for ZLD13, ZLD14, ZLD15, and ZLD16 respectively, which is consistent with the trend of J_{sc} values in Table 3.

Dye loading experiments has been conducted to correlate to device performance. According to Beer-Lambert law and the molar extinction coefficient of each dye (Table 3), dye adsorbed amounts for ZLD14 (2.3×10^{-7} mol/cm²) and ZLD16 (2.8×10^{-7} mol/cm²) are less than that for ZLD13 (3.1×10^{-7} mol/cm²) and ZLD15 (3.8×10^{-7} mol/cm²), respectively, which may be attributed from destroying the ordered arrangement of dye molecules after replacing 4-ethylbenzoic acid (within ZLD13 and ZLD15) with 5-ethylthiophene-2-carboxylic acid (within ZLD14 and ZLD16) as the electron acceptor. Destroying the ordered arrangement of dye molecules is advantaged to the suppression of charge recombination in DSSCs, which is consistent with the following electrochemical impedance study.

Dark current of DSSCs

In addition to absorption band, dark current or regeneration rate may also affect photovoltaic performance of DSSCs.¹⁹ To elucidate the factors affecting the performance of the cells, dark currents of DSSCs fabricated were checked (Fig. 6). Dark current of the cell of ZLD14 is slightly higher than ZLD13, which is consistent with the V_{oc} values listed in Table 3. Meanwhile, the DSSC of ZLD15 and ZLD16 exhibited significantly higher dark currents compared with ZLD13 and ZLD14, which is also consistent with photovoltaic performances listed in Table 3. These results indicate that dark current is an important factor to affect the photovoltaic performance of DSSCs here.

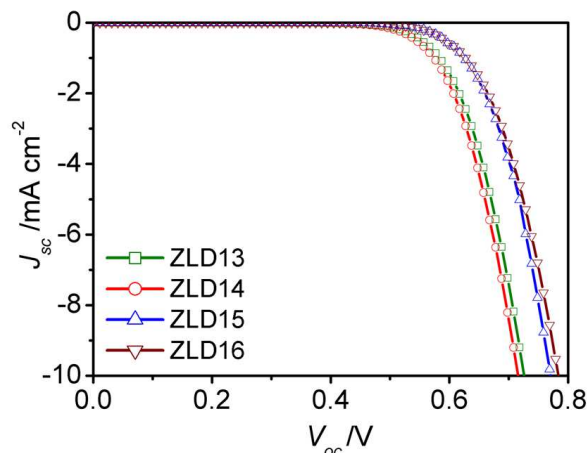


Fig. 6 Dark current of DSSCs based on ZLD13~ZLD16.

Electrochemical impedance spectroscopy

Electrochemical impedance spectrum (EIS) is a powerful tool to characterize the important interfacial charge transfer processes in the DSSCs.²⁰ Electrochemical impedance spectra were collected for each cell under illumination of AM 1.5G full sunlight (100 mW/cm²) and under dark. Two semicircles were observed in the Nyquist plots, which are assigned to the charge transfer at Pt/electrolyte interface (left peaks) and dye/TiO₂/electrolyte

interface (right peaks).^{20c-20f} The results generated from the EIS experiments have been summarized in Table 4.

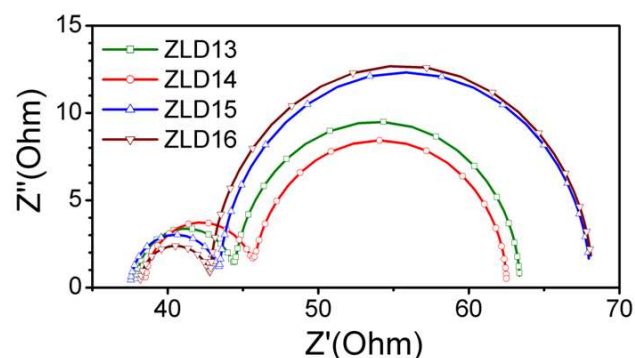


Fig. 7 Nyquist plots of Electrochemical Impedance Spectroscopy of DSSCs based on ZLD13~ZLD16 (under AM 1.5G full sunlight), scanned from 10^5 to 1 Hz. The applied potential and ac amplitude were set at open-circuit condition and 10 mV, respectively.

Nyquist plots and Bode phase plots of DSSCs, tested under AM 1.5G full sunlight, are shown in Fig. 7 and Fig. S3 of Supporting Information, respectively. The charge recombination resistance (R_{rec}) on the TiO₂ surface, which is related to the charge recombination rate between injected electron and electron acceptor (I_3^-) in the electrolyte,^{20d,20e} is estimated by the large semicircle width. A large R_{rec} means the small charge recombination rate and vice versa. The R_{rec} values of ZLD13~ZLD16 increase in the order of ZLD14 < ZLD13 < ZLD15 < ZLD16, which is consistent with the V_{oc} values listed in Table 3. These EIS results indicate that charge recombination is another important factor to affect the photovoltaic performance of DSSCs here.

Table 4 The detailed parameters extracted from electrochemical impedance spectra of DSSCs under AM 1.5G full sunlight and under dark respectively based on ZLD13~ZLD16.^a

Dye	Under light (AM 1.5G)		Under dark	
	$R_p(\Omega/\text{cm}^2)^b$	$R_{rec}(\Omega/\text{cm}^2)^c$	$R_p(\Omega/\text{cm}^2)^b$	$R_{rec}(\Omega/\text{cm}^2)^c$
ZLD13	6	19	9	38
ZLD14	8	17	9	25
ZLD15	7	25	8	57
ZLD16	5	26	8	64

^aAll the devices are based on 4×4 mm TiO₂ thin films (ca. 12 μm), using 0.6 M DMII, 50 mM LiI, 30 mM I₂, 0.5 M tert-butylpyridine and 0.1 M GuNCS in acetonitrile and valeronitrile (85 : 15) as the electrolyte. ^b R_p represents the charge-transfer resistance at the Pt and FTO glass. ^c R_{rec} represents the charge-transfer resistance at the dye/TiO₂/electrolyte interface related to electron recombination.

Nyquist plots and Bode phase plots of DSSCs tested under dark are shown in Fig. S4 and Fig. S5 of Supporting Information, respectively. The intermediate frequency semicircle in the electrochemical impedance spectra represents the charge transfer phenomena between the dye/TiO₂/electrolyte interface under dark. Efficient suppression of the dark current leads to larger semicircle. The resistance towards the dark current (the size of semicircle) also increases in the order of ZLD14 < ZLD13 < ZLD15 < ZLD16. Therefore, the aforementioned arguments on dark current were supported by the electrochemical impedance spectroscopic (EIS) studies carried out in the dark.

3. Conclusions

In this paper, we adopt two moieties, namely 4,4'-di(2-thienyl)triphenylamine and 5-ethynylthiophene-2-carboxylic acid, as electron push and pull moieties of porphyrin sensitizer for the first time on the basis of theoretical calculation. Four porphyrin dyes, named ZLD13, ZLD14, ZLD15 and ZLD16, were synthesized and fully characterized. After introducing one above moiety to fundamental dye ZLD13, the energy conversion efficiencies (η) are improved in different degrees, demonstrating the effectiveness of our structure modification methods. When two moieties were both introduced, η is further enhanced (ZLD16), which is comparable with N719-based reference cell

Notes and references

^aState Key Laboratory of Coordination Chemistry, School of Chemistry and Chemical Engineering, Nanjing National Laboratory of Microstructures, Nanjing University, Nanjing 210093, P. R. China, E-mail: zhenghg@nju.edu.cn. Fax : 86-25-83314502.

^bInstitute of Theoretical and Computational Chemistry, Key Laboratory of Mesoscopic Chemistry of Ministry of Education, School of Chemistry and Chemical Engineering, Nanjing University, Nanjing 210093, P. R. China, E-mail: majing@nju.edu.cn.

^cState Key Laboratory of Materials-Oriented Chemical Engineering, College of Chemistry and Chemical Engineering, Nanjing University of Technology, Nanjing 210009, P. R. China, E-mail: zhouxf@njut.edu.cn.

† Electronic Supplementary Information (ESI) available: Preparation details of dyes, experimental section, ATR-FTIR spectra, Nyquist plots and Bode phase plots of EIS. See DOI: 10.1039/b000000x/

1. (a) M. Liang, J. Chen, *Chem. Soc. Rev.*, 2013, **42**, 3453; (b) B. E. Hardin, H. J. Snaith and M. D. McGehee, *Nat. Photonics*, 2012, **6**, 162; (c) C. Risko, M. D. McGehee and J. L. Bredas, *Chem. Sci.*, 2011, **2**, 1200; (d) Y. Bai, J. Zhang, D. Zhou, Y. Wang, M. Zhang and P. Wang, *J. Am. Chem. Soc.*, 2011, **133**, 11442; (e) B. O'Regan, M. Grätzel, *Nature*, 1991, **353**, 737; (f) X. Yang, M. Yanagida and L. Han, *Energy Environ. Sci.*, 2013, **6**, 54; (g) A. Hagfeldt, G. Boschloo, L. Sun, L. Kloo and H. Pettersson, *Chem. Rev.*, 2010, **110**, 6595; (h) J. Wu, Y. Xiao, G. Yue, Q. Tang, J. Lin, M. Huang, Y. Huang, L. Fan, Z. Lan, S. Yin, T. Sato, *Adv. Mater.*, 2012, **24**, 1884.
2. (a) S. K. Balasingam, M. Lee, M. G. Kang and Y. Jun, *Chem. Commun.*, 2013, **49**, 1471; (b) J. Y. Liu, D. F. Zhou, M. F. Xu, X. Y. Jing and P. Wang, *Energy Environ. Sci.*, 2011, **4**, 3545.
3. (a) L.-L. Li, E. W.-G. Diau, *Chem. Soc. Rev.*, 2013, **42**, 291; (b) C.-L. Wang, C.-M. Lan, S.-H. Hong, Y.-F. Wang, T.-Y. Pan, C.-W. Chang, H.-H. Kuo, M.-Y. Kuo, E. W.-G. Diau and C.-Y. Lin, *Energy Environ. Sci.*, 2012, **5**, 6933; (c) H. Imahori, T. Umeyama, K. Kurotobi and Y. Takano, *Chem. Commun.*, 2012, **48**, 4032.
4. (a) T. Bessho, S. M. Zakeeruddin, C. Y. Yeh, E. W. G. Diau and M. Grätzel, *Angew. Chem., Int. Ed.*, 2010, **49**, 6646; (b) W. M. Campbell, K. W. Jolley, P. Wagner, K. Wagner, P. J. Walsh, K. C. Gordon, L. Schmidt-Mende, M. K. Nazeeruddin, Q. Wang, M. Grätzel and D. L. Officer, *J. Phys. Chem. C*, 2007, **111**, 11760; (c) Y. C. Chang, C. L. Wang, T. Y. Pan, S. H. Hong, C. M. Lan, H. H. Kuo, C. F. Lo, H. Y. Hsu, C. Y. Lin and E. W. Diau, *Chem. Commun.*, 2011, **47**, 8910.
5. (a) C.-Y. Lin, C.-F. Lo, L. Luo, H.-P. Lu, C.-S. Hung and E. W.-G. Diau, *J. Phys. Chem. C*, 2009, **113**, 755; (b) C.-W. Lee, H.-P. Lu, C.-M. Lan, Y.-L. Huang, Y.-R. Liang, W.-N. Yen, Y.-C. Liu, Y.-S. Lin, E. W.-G. Diau and C.-Y. Yeh, *Chem.-Eur. J.*, 2009, **15**, 1403.
6. T. Bessho, S. Zakeeruddin, C. Y. Yeh, E. G. Diau and M. Grätzel, *Angew. Chem., Int. Ed.*, 2010, **49**, 6646.
7. A. Yella, H.-W. Lee, H. N. Tsao, C. Yi, A. K. Chandiran, M. K. Nazeeruddin, E. W.-G. Diau, C.-Y. Yeh, S. M. Zakeeruddin and M. Grätzel, *Science*, 2011, **334**, 629.
8. Y.-S. Yen, H.-H. Chou, Y.-C. Chen, C.-Y. Hsu and J. T. Lin, *J. Mater. Chem.*, 2012, **22**, 8734.
9. M. D. Zhang, H. Pan, X. H. Ju, Y. J. Ji, L. Qin, H. G. Zheng and X. F. Zhou, *Phys. Chem. Chem. Phys.*, 2012, **14**, 2809.
10. T. Ripolles-Sanchis, B.-C. Guo, H.-P. Wu, T.-Y. Pan, H.-W. Lee, S. R. Raga, F. Fabregat-Santiago, J. Bisquert, C.-Y. Yeh and E. W.-G. Diau, *Chem. Commun.*, 2012, **48**, 4368.
11. DFT calculations were performed using Gaussian 09 program: Gaussian 09, Revision B.01, M. J. Frisch, G. W. Trucks, H. B. Schlegel, G. E. Scuseria, M. A. Robb, J. R. Cheeseman, G. Scalmani, V. Barone, B. Mennucci, G. A. Petersson, H. Nakatsuji, M. Caricato, X. Li, H. P. Hratchian, A. F. Izmaylov, J. Bloino, G. Zheng, J. L. Sonnenberg, M. Hada, M. Ehara, K. Toyota, R. Fukuda, J. Hasegawa, M. Ishida, T. Nakajima, Y. Honda, O. Kitao, H. Nakai, T. Vreven, Jr. J. A. Montgomery, J. E. Peralta, F. Ogliaro, M. Bearpark, J. J. Heyd, E. Brothers, K. N. Kudin, V. N. Staroverov, T. Kieth, R. Kobayashi, J. Normand, K. Raghavachari, A. Rendell, J. C. Burant, S. S. Iyengar, J. Tomasi, M. Cossi, N. Rega, N. J. Millam, M. Klene, J. E. Knox, J. B. Cross, V. Bakken, C. Adamo, J. Jaramillo, R. Gomperts, R. E. Stratmann, O. Yazyev, A. J. Austin, R. Cammi, C. Pomelli, J. W. Ochterski, R. L. Martin, K. Morokuma, V. G. Zakrzewski, G. A. Voth, P. Salvador, J. J. Dannenberg, S. Dapprich, A. D. Daniels, Farkas, J. B. Foresman, J. V. Ortiz, J. Cioslowski, and D. J. Fox, Gaussian, Inc., Wallingford CT, 2010.
12. K. Hara, Y. Dan-oh, C. Kasada, Y. Ohga, A. Shinpo, S. Suga, K. Sayama and H. Arakawa, *Langmuir*, 2004, **20**, 4205.
13. (a) J. K. Lee, S. M. Lee, S. B. Lee, K. H. Kima, S. E. Cho, S. Jang, S. H. Park, W. P. Hwang, M. H. Seo and M. R. Kima, *Curr. Appl. Phys.*, 2011, **11**, S140; (b) M. Liang, W. Xu, F. Cai, P. Chen, B. Peng, J. Chen and Z. Li, *J. Phys. Chem. C*, 2007, **111**, 4465.
14. (a) L. Y. Lin, C. H. Tsai, K. T. Wong, T. W. Huang, L. Hsieh, S. H. Liu, H. W. Lin, C. C. Wu, S. H. Chou, S. H. Chen and A. I. Tsai, *J. Org. Chem.*, 2010, **75**, 4778; (b) C. Klein, M. K. Nazeeruddin, D. D. Censo, P. Liska and M. Grätzel, *Inorg. Chem.* 2004, **43**, 4216.
15. Y. C. Chen, H. H. Chou, M. C. Tsai, S. Y. Chen, J. T. Lin, C. F. Yao and K. Chen, *Chem. Eur. J.*, 2012, **18**, 5430.
16. (a) K. Kalyanasundaram, M. Grätzel, *Coord. Chem. Rev.*, 1998, **77**, 347; (b) S. Ito, P. Chen, P. Comte, M. K. Nazeeruddin, P. Liska, P. Péchy and M. Grätzel, *Prog. Photovolt: Res. Appl.*, 2007, **15**, 603; (c) S. Ito, T. N. Murakami, P. Comte, P. Liska, C. Grätzel, M. K. Nazeeruddin and M. Grätzel, *Thin Solid Films*, 2008, **516**, 4613.
17. (a) H. S. Yang, Y. S. Yen, Y. C. Hsu, H. H. Chou and J. T. Lin, *Org. Lett.*, 2010, **12**, 16; (b) P. Wang, S. M. Zakeeruddin, P. Comte, R. Charvet, R. Humphry-Baker and M. Grätzel, *J. Phys. Chem. B*, 2003, **107**, 14336.
18. Q. Wang, S. Ito, M. Grätzel, F. Fabregat-Santiago, I. Mora-Sero, J. Bisquert, T. Bessho and H. Imai, *J. Phys. Chem. B*, 2006, **110**, 25210.
19. Y. C. Chen, H. H. Chou, M. C. Tsai, S. Y. Chen, J. T. Lin, C. F. Yao and K. Chen, *Chem. Eur. J.*, 2012, **18**, 5430.

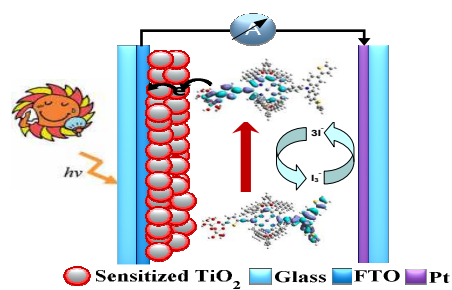
20. (a) Z. S. Wang, K. Sayama and H. Sugihara, *J. Phys. Chem. B*, 2005, **109**, 22449; (b) P. Shen, Y. Tang, S. Jiang, H. Chen, X. Zheng, X. Wang, B. Zhao, S. Tan, *Org. Electron.*, 2011, **12**, 125; (c) C. Longo, A. F. Nogueira and M. D. Paoli, *J. Phys. Chem. B*, 2002, **106**, 5925;
- 5 (d) R. Kern, R. Sastrawan, J. Ferber, R. Stangl and J. Luther, *Electrochim. Acta*, 2002, **47**, 4213; (e) E. Kozma, I. Concina, A. Braga, L. Borgese, L. E. Depero, A. Vomiero, G. Sberveglieri and M. Catellani, *J. Mater. Chem.*, 2011, **21**, 13785; (f) Z. Ji, G. Natu, Z. J. Huang and Y. Y. Wu, *Energy Environ. Sci.*, 2011, **4**, 2818.
- 10

Manuscript ID TA-ART-05-2014-002335

Title: Promising alkoxy-wrapped porphyrins with novel push-pull moieties for dye-sensitized solar cells

The table of contents entry:

Colour graphic:



Text:

This paper focuses on the structure modification of sensitizers for efficient porphyrin-sensitized solar cells (PSSCs).